RSC Advances

PAPER

View Article Online
View Journal | View Issue



Cite this: *RSC Adv.*, 2014, **4**, 8044

# Photoinduced solid state keto–enol tautomerization of 2-(2-(3-nitrophenyl)-4,5-diphenyl-1*H*-imidazol-1-yloxy)-1-phenylethanone†

Arun Kumar Padhy,*[a] Ashok K. Mishra,[b] Monalisa Mohapatra,[b] Avik Kumar Pati[b] and Sasmita Mishra[c]

Received 10th September 2013
Accepted 18th November 2013

DOI: 10.1039/c3ra44948c

www.rsc.org/advances

Excited state intramolecular proton transfer (ESIPT) plays an important role in biological systems and has also recently found applications in electronic devices such as transducers, switches *etc.* In this paper we report the synthesis and solid state photochromic behavior of 2-(2-(3-nitrophenyl)-4,5-diphenyl-1*H*-imidazol-1-yloxy)-1-phenylethanone (**II**) due to ESIPT. Compound **II** exhibits yellow color in dark and red color in light, with the yellow form attributed to the keto derivative and the red form assigned to its enol derivative The color change in the presence of light is thus attributed to the keto–enol tautomerism through ESIPT. The color change from yellow to red is a photochemical process which thermally decays to the yellow form in the dark. The solid state stability of the enol form upon phototautomerization of the keto form is a noteworthy phenomenon, and its stability has been substantiated by our experimental findings. In the solution state, the yellow form (keto) is stable in chloroform while the red form (enol) is stable in DMSO. Theoretical calculations have been performed to understand the geometries and electronic transitions of the keto and enol forms. In addition, ground and excited state equilibrium constants for the keto–enol tautomerism were calculated.

In recent years, the structural switchability of organic molecules from one form to another by external stimuli such as heat,[1] redox potential,[2] pH[3] or light[4] has received much attention. Among these, light helps the efficient conversion as it leads to a clean reaction without any by-products. Excited state intramolecular proton transfer (ESIPT) commonly initiated by photons or light is often observed in keto–enol tautomerism and is important in several areas of biochemistry. For example, the high phosphate transfer potential of phosphoenolpyruvate results from the fact that the phosphorylated compound is trapped in the less stable enol form, whereas after dephosphorylation it can assume the keto form. Rare enol tautomers of the bases guanine and thymine can lead to mutations because of their altered base pairing properties. The semi-empirical method of measuring[5] the effect of acetaldehyde and ethyl–methyl ketone tautomerism at room temperature on chemical nanotube sensors reveals that the keto structure is more stable because of intramolecular H-bonds.

The photochromic keto–enol tautomerism of Schiff bases derived from 2-hydroxyaldehyde, with a hydrogen intramolecular bond in the *cis*-enol form[6], leads to its possible applications in optical switch devices which are advantageous in rapid transfer reactions[7] and high photochemical fasteners.[8,9] The existence of an imidazole ring in 2′-deoxyisoguanosine[10] favors the enol form with the restoration of the aromaticity.

Keto–enol tautomerism through ESIPT has been studied extensively for diketones and triketones. In most cases, it has been observed that the proton transfer is solvent-dependent and the keto form is primarily found in more polar solvents, while the enol form is observed in non-polar solvents. The profound existence of the keto form in polar solvents is attributed to the dipole polarizability of the solvent rather than the dipole moment of the solvent. However, in some Schiff's bases,[11] it has been observed that the enol form predominantly exists in polar solvents.

At this juncture, we thought that in order to achieve the reversibility in a controlled and predictable manner, tuning of the molecular structure is essential, which can modify the properties precisely. This tuning of the molecular structure can be achieved by suitably modifying the functionality of the

[a]*Centre for Applied Chemistry, Central University of Jharkhand, Ranchi-835205, India. E-mail: arun_nist@hotmail.com; Fax: +91-6531-294161; Tel: +91-9437067761*

[b]*Department of Chemistry, Indian Institute of Technology, Madras, Chennai, India. E-mail: mishra@iitm.ac.in; Fax: +91-44-22574202; Tel: +91-44-22574207*

[c]*Department of Chemistry, National Institute of Technology, Rourkela, Orissa, India*

† Electronic supplementary information (ESI) available: general experimental methods, synthetic procedures, characterization data, spectra, and cartesian co-ordinates for optimized geometry. See DOI: 10.1039/c3ra44948c

molecule, which can lead to switching back and forth in response to external stimuli. Because light can be easily tuned and focused, it is a particularly appealing stimulus to trigger changes in the structure of molecules, and can be used with a wide range of materials, as well as in both the solution and solid state.[12]

Thus, in continuation of our work, herein we report the synthesis and solid state photochromic behavior of 2-(2-(3-nitrophenyl)-4,5-diphenyl-1*H*-imidazol-1-yloxy)-1-phenylethanone through keto–enol tautomerism. In addition to its solid state photochromic behavior, the solution state photophysical properties of the derivative **II** have also been explored. Theoretical investigations have been carried out to understand the electronic structure of both the keto and enol forms of the derivative **II**, to comprehend their solution phase stability. Equilibrium constant calculations of the keto–enol tautomerism and computations of electronic transitions for the keto and enol forms have been carried out to understand the thermochemistry and photophysics respectively.

## Results & discussion

The synthesis and crystal structure of $N_1$-hydroxy imidazoles[13] have been reported previously from our laboratory. In an attempt to improvise the metal binding ability and to explore the possibility of thermal cleavage to form a keto-aldehyde, we have synthesized the phenacyl derivative of the said imidazole.

Compound **II** was prepared by the reaction of the imidazole (**I**) with 2-bromo-1-phenylethanone (commonly known as phenacyl bromide) in acetone in the presence of a mild base (Scheme 1). Under ambient light conditions in the laboratory, the precipitated solid was red in color. To our surprise, it was found that it turned yellow when kept overnight in the dark, but immediately turned red when exposed to light. The change in color of the solid from yellow to red was found to be spontaneous and was complete within a couple of minutes on exposure to diffused sunlight, whereas the reverse change took more than 24 h in the dark. The baseline-corrected DRS (Diffuse Reflectance Spectroscopy) spectra were used to understand the origin of the yellow and red color of the derivative **II** in the two different forms (Fig. 1). It is observed that the yellow form absorbs significantly in the blue (400–450 nm) region, as expected. The red form shows appreciable light absorption in the blue and green region (400–600 nm), thereby appearing in its complementary red color.

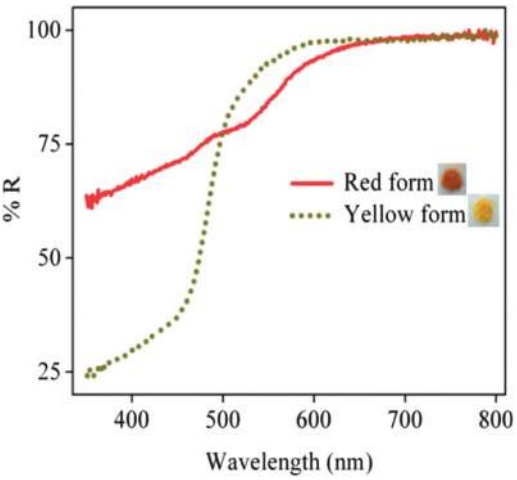


Fig. 1 Baseline-corrected DRS spectra of the yellow and red forms of the compound.

Compound **II** was found to show very poor solubility in most of the solvents. When the solid compound was dissolved in solvents like $CHCl_3$, the solution was yellow in color; however it appeared red in the more polar DMSO. This indicates the presence of two different species in the respective solvents, as observed in the case of benzodifurantrione.[14] In order to look into the existence of any structural changes in the compound in both the solvents, NMR studies were performed in DMSO-$d_6$ and $CDCl_3$. The solution phase NMR spectrum in $CDCl_3$ has significant peaks at $\delta$ 4.9 corresponding to the $-CH_2$ protons, and $\delta$ 8.2 for the *ortho* proton of the phenyl group attached to the carbonyl carbon, which is due to the diamagnetic anisotropy of the carbonyl group. The $^{13}C$ spectrum has peaks at 190 ppm for the carbonyl carbon and 79.3 ppm for the methylene carbon. On the other hand, in DMSO-$d_6$ solution, the $^1H$ NMR spectrum has peaks at $\delta$ 5.69 (–CH) and $\delta$ 8.07 (both the ortho protons). Obtaining a clear $^{13}C$ NMR spectrum was difficult because of its poor solubility. Only in DMSO, where the compound solubility is good, does the enolic form exist. The $^{13}C$ spectrum similarly exhibits carbons resonating at 89 ppm (–C=CH) and 196.89 ppm (–C(OH)=C). The high downfield shift for the enolic carbon to 196.89 is a well-known and established consequence of the formation of a H-bonded ring structure of the enolic hydroxyl group with the neighboring electronegative atoms.[15] The existence of a trace amount of ketone in the enol form, however, cannot be overruled completely. The DEPT (Distortionless Enhancement by Polarization Transfer) study of the $^{13}C$ NMR revealed that in DMSO, which is polar, the red-colored enol form exists, and in chloroform the yellow-colored keto form exists. Any advanced NMR studies, such as low temperature NMR, turn out to be ineffective as the compound precipitates out at low temperature.[16] Even cross polarization-magic angle spinning (CP-MAS) solid state NMR experiments of both the yellow and red forms did not reveal any useful information, owing to the presence of significant noise and a high spectral

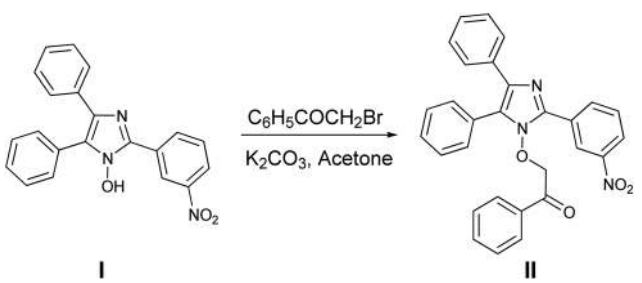


Scheme 1 Synthesis of the phenacyl derivative.

bandwidth, merging all of the aromatic signals together (see ESI†).

In order to know more about the color change; solution phase absorption and transmittance studies were carried out in DMSO and $CHCl_3$. Fig. 2A represents the absorption spectra of the compound ($10^{-5}$ M) in DMSO and $CHCl_3$. This shows a slight red shift in the absorption maximum in the more polar DMSO solvent. This small red shift appears to be due to the DEPT observation that the compound is in its enolic form in DMSO. In order to understand the origin of the color in $CHCl_3$ and DMSO, transmittance spectra of the concentrated solutions (2 mM of the compound) were recorded. Fig. 2B shows the transmittance spectra of the compound (2 mM) in DMSO and $CHCl_3$. It is observed that the keto form in $CHCl_3$ absorbs significantly in the blue (400–450 nm) region, meaning it is visualized as its complementary yellow color. However, the enol form in DMSO absorbs entirely in the blue and green (400–600 nm) region, causing it to be visualized as its complementary red color.

The close similarity of the transmittance spectra of the yellow and red forms in the solid state and in solution suggests that in the solid state the yellow color could arise from the keto form and the red color from the enol form. Based on the above observations, the yellow-to-red form conversion of the derivative **II** in the solid state upon exposure to light was designated as photoinduced keto–enol tautomerism, as indicated in Scheme 2. The enol form claims special importance owing to its high stability in the solid state.

Other mechanisms, such as cyclization involving proton transfer, are ruled out as the aromatic ring at the 2-position has to lose its aromaticity, which is unlikely, and also on the grounds of the NMR experiments, no such peaks are observed corresponding to the aliphatic carbon.

Further, the electronic structures of the keto and enol forms were investigated through B3LYP/6-311+G(d,p) density functional theory (DFT)[17,18] calculations using the Gaussian 09 computational program.[19] The ground state optimized geometries of the keto and enol forms are depicted in Fig. 3. In the keto form, the three phenyl groups attached to the central five-membered heterocyclic ring are out of the plane of the five-membered ring and are propeller-shaped. In the enol form, the three phenyl rings attached to the five-membered ring also follows the same geometry as the keto form. The noteworthy feature of the enol form is that the enolic olefin is *trans* in geometry and the enolic hydrogen is *anti* to the nitro substituted phenyl ring, presumably to avoid steric crowding with the hydrogen of the nitro-substituted phenyl ring.

The first vertical absorption ($S_0 \rightarrow S_1$) for both the keto and enol forms involves a HOMO → LUMO transition (Table 1). Table 1 depicts the oscillator strength, vertical excitation energies and orbital contributions for the keto and enol forms in the gas phase, $CHCl_3$ and DMSO. As we move from the gas phase to $CHCl_3$ to DMSO, the vertical excitation energy decreases. This implies that polar solvents stabilize the HOMO and LUMO and thereby help to reduce the vertical excitation energy. The excitation energy of the enol form is less than that of the keto form in a particular solvent, indicating greater solvent stabilization of the HOMO and LUMO of the enol form than of the keto derivative. The HOMO of the keto form comprises of the core five-membered heterocyclic ring, two unsubstituted phenyl rings attached to the five-membered ring and the phenyl ring of the nitro-substituted phenyl moiety, while the LUMO includes the whole nitro-substituted phenyl moiety (Fig. 4a). The pendant oxygen-substituted phenacyl group does not contribute to the electronic distributions of the HOMO and LUMO in the keto form.

Earlier, we discussed that the keto form is converted into the enol form in highly polar solvents such as dimethyl sulfoxide (DMSO). This observation urges us to look at the electronic structure of the enol form, where the pendant oxygen-substituted group should play an important role in electronic

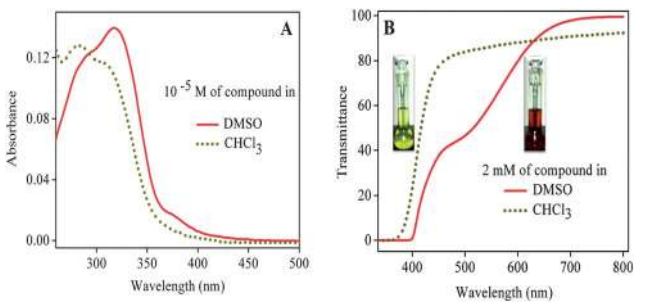


Fig. 2 (A) Absorption and (B) transmittance spectra of the compound in DMSO and $CHCl_3$.

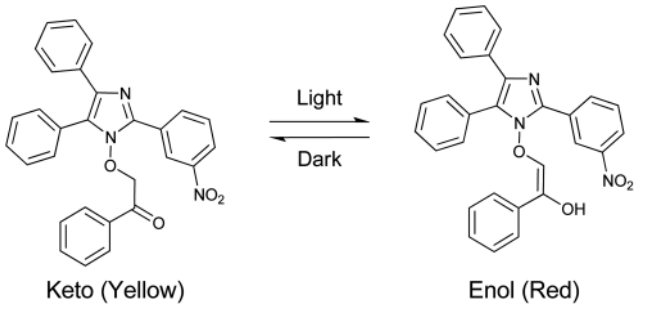


Scheme 2 Suggested keto–enol transformation.

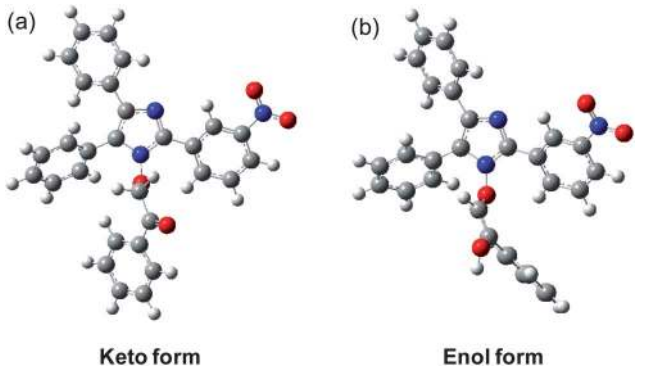


Fig. 3 Ground state optimized geometry of the (a) keto form and (b) enol form in the gas phase.

Table 1 1st vertical excitation energy, oscillator strength, and orbital transition using B3LYP/6-311+G**

| Gas phase/solvents | Keto–enol forms | Vertical excitation energy (eV) | Oscillator strength (f) | Orbital transitions |
|---|---|---|---|---|
| Gas phase | Keto | 2.8059 | 0.0123 | HOMO → LUMO (99.10%) |
| | Enol | 2.7508 | 0.0125 | HOMO → LUMO (99.14%) |
| $CHCl_3$ | Keto | 2.5386 | 0.0102 | HOMO → LUMO (99.30%) |
| | Enol | 2.5047 | 0.0102 | HOMO → LUMO (99.32%) |
| DMSO | Keto | 2.4540 | 0.0081 | HOMO → LUMO (99.33%) |
| | Enol | 2.4321 | 0.0082 | HOMO → LUMO (99.35%) |

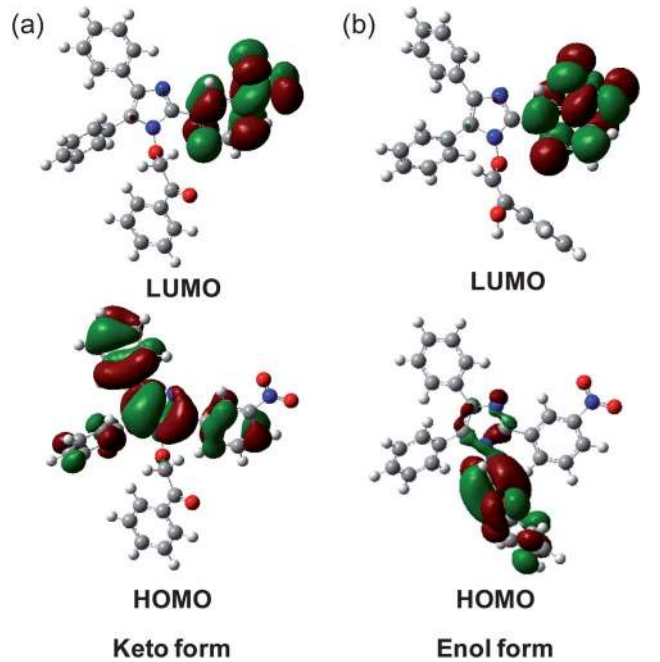


Fig. 4 HOMO and LUMO of the (a) keto form and (b) enol form.

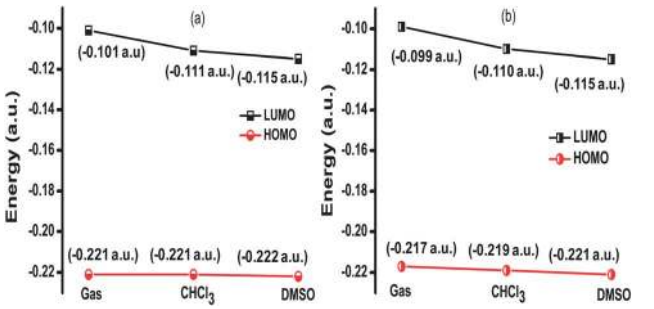


Fig. 5 HOMO and LUMO energy in the gas phase, $CHCl_3$ and DMSO for the (a) keto and (b) enol forms.

Table 2 Energy of the keto and enol forms in the ground state in the gas phase, $CHCl_3$ and DMSO

| | Energy ($E$ in a.u.) without zero point vibrational energy correction | |
|---|---|---|
| Gas phase/solvents | Keto form ($E_{keto}$) | Enol form ($E_{enol}$) |
| Gas phase | −1583.14671150 | −1583.12688970 |
| $CHCl_3$ | −1583.160152922 | −1583.14003841 |
| DMSO | −1583.16662593 | −1583.14570805 |

distribution. The LUMO of the enol form resembles the LUMO of the keto form, whereas the HOMO is contributed by the pendant oxygen-substituted enolized phenacyl moiety, as anticipated (Fig. 4b). With the ketone group being enolized, the electron density in the HOMO of the enol form is mainly localized on the electron-rich enolic moiety.

The HOMO and LUMO energy stabilization of the keto and enol forms was studied in the gas phase and in chloroform and dimethyl sulfoxide media (Fig. 5). Both the HOMO and LUMO of the keto and enol forms are stabilized from gas to chloroform to DMSO. The stabilization of the HOMO of the enol form is twice that of the keto form, when going from chloroform to DMSO. At this point, it is worth stressing that although the HOMO and LUMO of the enol form are stabilized from the gas phase to solvent phase relative to the keto form, the overall stability of the keto form is higher than the enol form in the gas phase and in the solvents (Table 2). Thus, the experimental observation of the red color of derivative **II** in DMSO may be attributed to the certain percentage of the enol form present in the keto–enol tautomerism reaction in the ground state.

In an effort to understand the equilibrium constant of the keto–enol tautomerism in the ground state, the thermochemical parameters such as the enthalpy change ($\Delta H$), free energy change ($\Delta G$) and entropy change ($\Delta S$) were computed. It was found that the keto form is more stable in the ground state, and the equilibrium constant of the keto–enol tautomerism was noted to be low (Table 3).

Earlier, we observed that the keto form is transformed into the enol very quickly upon irradiation with light. Thus, the equilibrium constant of the keto*–enol* tautomerism in the excited state is expected to be high. Considering the high computational cost to optimize the keto and enol forms of the derivative **II** in the excited state, we adopted a thermochemical energy diagram (Scheme 3) to estimate the excited state free energy change of the keto*–enol* tautomerism to obtain its equilibrium constant. Although the values obtained in this way are approximate, they can provide valuable insight into the photochromic process.

It was assumed that the transition energy is close to the changes in internal energy, assuming the work related to

Table 3 Thermochemical parameters for the keto–enol tautomerism

| | Keto ⇌ enol tautomerism in the ground state | | | |
|---|---|---|---|---|
| Gas phase/solvents | $\Delta H$ (kcal mol$^{-1}$) | $\Delta S$ (kcal mol$^{-1}$) | $\Delta H$ (kcal mol$^{-1}$) | $K_{eq}$ |
| Gas phase | 12.1235 | −0.001012 | 12.4252 | $7.78 \times 10^{-10}$ |
| $CHCl_3$ | 13.1539 | 0.006544 | 11.2028 | $6.13 \times 10^{-9}$ |
| DMSO | 13.4262 | 0.006064 | 11.6182 | $3.04 \times 10^{-9}$ |

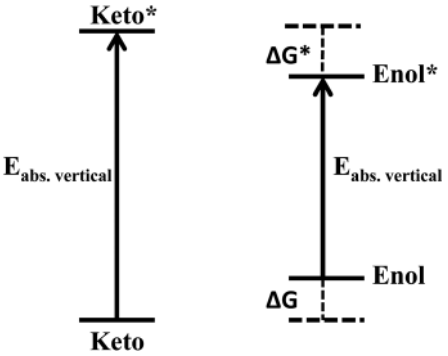


Scheme 3 Thermochemical energy diagram for the keto–enol tautomerism.

volume expansion to be negligible and the entropy changes of the different states of the molecules to be insignificant. Thus, $\Delta E_{abs.vertical}$ for keto → keto* and enol → enol* was considered from Table 1, and $\Delta G$ was assumed to be equivalent to $\Delta H$, neglecting $\Delta S$. The free energy change in the excited state $\Delta G^*$ for the keto*–enol* tautomerism was calculated to be −11.728, −12.372 and −12.921 kcal mol$^{-1}$ in the gas phase, $CHCl_3$ and DMSO respectively. Thus, the $K^*_{eq}$ for the keto*–enol* tautomerism was found to be $3.96 \times 10^8$, $1.17 \times 10^9$ and $2.97 \times 10^9$ in the gas phase, $CHCl_3$ and DMSO respectively. The negative value of $\Delta G^*$ and the high value of $K^*_{eq}$ indicate that the enol* form is more stable than the keto* form.

## Conclusions

In summary, we have described the solid state keto–enol tautomerization of 2-(2-(3-nitrophenyl)-4,5-diphenyl-1*H*-imidazol-1-yloxy)-1-phenyl-ethanone (**II**). The initial color change (keto → enol) is a photo-initiated process and quite fast, whereas the reverse color change (enol → keto) is a thermal process and quite slow, which was corroborated theoretically through the calculations of the ground and excited state equilibrium constants for the keto–enol and keto*–enol* tautomerism respectively. The ESIPT from the keto form to the enol form is photochemically controlled, and the enol then thermodynamically decays to the keto form. The enol form of the derivative **II** is attractive because of its high stability in the solid state. As observed, the dark reaction took more than 24 h, suggesting that the energy is retained for a longer period of time. Thus, we believe that this concept could be useful for applications in molecular memory devices.

## Acknowledgements

One of the authors, A. K. Padhy, is thankful to INSA for awarding the visiting fellowship, to carry out some work at IIT Madras. The authors are also thankful to IIT Madras for the instrumental facilities. The high performance computing facility of IIT Madras is greatly acknowledged.

## References

1 D. Zhao, D. Q. Yuan, R. Krishna, J. M. van Baten and H. C. Zhou, *Chem. Commun.*, 2010, **46**, 7352–7354.
2 T. D. Nguyen, H. R. Tseng, P. C. Celestre, A. H. Flood, Y. Liu, J. F. Stoddart and J. I. Zink, *Proc. Natl. Acad. Sci. U. S. A.*, 2005, **102**, 10029–10034.
3 C. Park, K. Oh, S. C. lee and C. Kim, *Angew. Chem., Int. Ed.*, 2007, **46**, 1455–1457.
4 S. Yagai and A. Kitamura, *Chem. Soc. Rev.*, 2008, **37**, 1520–1529.
5 M. Monajjemi, L. Mahdavian, F. Mollaamin and B. Honarparvar, *Fullerenes, Nanotubes, Carbon Nanostruct.*, 2010, **18**, 45–55.
6 E. Hodjoudis, *J. Photochem.*, 1981, **17**, 355–366.
7 H. Durr, *Angew. Chem., Int. Ed. Engl.*, 1989, **28**, 413–431.
8 R. S. Becker, C. Lenoble and A. Zein, *J. Phys. Chem.*, 1987, **91**, 3509–3517.
9 R. V. Andres and D. M. Manikovski, *Appl. Opt.*, 1968, **7**, 1179–1183.
10 T. A. Martinof and S. A. Benner, *J. Org. Chem.*, 2004, **69**, 3972–3975.
11 M. Rospenk, I. Krol-starzomska, A. Filarowski and A. Koll, *Chem. Phys.*, 2003, **287**, 113–124.
12 *Organic Photochromic & Thermochromic Compounds*, ed. C. Crano and R. J. Gugielmetti, Plenum Press, New York, 1999.
13 A. K. Padhy, B. Chetia, S. Mishra, A. Pati and P. K. Iyer, *Tetrahedron Lett.*, 2010, **51**, 2751–2753.
14 A. J. Lawrence, M. G. Hutchings, A. R. Kennedy and J. J. W. McDouall, *J. Org. Chem.*, 2010, **75**, 690–701.
15 S.-H. An, *Arch. Pharmacal Res.*, 1986, **9**, 229–232; B. S. Min, B. S. Yu, H. K. Lee, H. J. Jung and J. S. Choi, *Bioorg. Med. Chem. Lett.*, 2006, **16**, 3255–3257; A. R. Katritzky, Z. Wang and C. D. Hall, *ARKIVOC*, 2008, **x**, 26–36; A. Mateskaa, G. Stojkovica, B. Mikhova, K. Mladenovska and E. Popvski, *ARKIVOC*, 2009, **x**, 131–140.
16 I. Alkorta, P. Goya, J. Elguero and S. P. Singh, *Natl. Acad. Sci. Lett.*, 2007, **30**, 139–159.

 

17 C. Lee, W. Yang and R. G. Parr, *Phys. Rev. B: Condens. Matter Mater. Phys.*, 1988, **37**, 785.
18 A. D. Becke, *J. Chem. Phys.*, 1993, **98**, 1372.
19 M. J. Frisch, G. W. Trucks, H. B. Schlegel, G. E. Scuseria, M. A. Robb, J. R. Cheeseman, G. Scalmani, V. Barone, B. Mennucci, G. A. Petersson, H. Nakatsuji, M. Caricato, X. Li, H. P. Hratchian, A. F. Izmaylov, J. Bloino, G. Zheng, J. L. Sonnenberg, M. Hada, M. Ehara, K. Toyota, R. Fukuda, J. Hasegawa, M. Ishida, T. Nakajima, Y. Honda, O. Kitao, H. Nakai, T. Vreven, J. A. Montgomery, J. E. Peralta, F. Ogliaro, M. Bearpark, J. J. Heyd, E. Brothers, K. N. Kudin, V. N. Staroverov, T. Keith, R. Kobayashi, J. Normand, K. Raghavachari, A. Rendell, J. C. Burant, S. S. Iyengar, J. Tomasi, M. Cossi, N. Rega, J. M. Millam, M. Klene, J. E. Knox, J. B. Cross, V. Bakken, C. Adamo, J. Jaramillo, R. Gomperts, R. E. Stratmann, O. Yazyev, A. J. Austin, R. Cammi, C. Pomelli, J. W. Ochterski, R. L. Martin, K. Morokuma, V. G. Zakrzewski, G. A. Voth, P. Salvador, J. J. Dannenberg, S. Dapprich, A. D. Daniels, O. Farkas, J. B. Foresman, J. V. Ortiz, J. Cioslowski and D. J. Fox, *Gaussian 09, Revision C.01*, Gaussian, Inc., Wallingford CT, 2010.